Monthly Notices
of the
ROYAL ASTRONOMICAL SOCIETY

Mon. Not. R. Astron. Soc. **413,** 2281–2287 (2011) doi:10.1111/j.1365-2966.2011.18306.x

Surface formation of CO_2 ice at low temperatures

S. Ioppolo,[1⋆] Y. van Boheemen,[1] H. M. Cuppen,[1,2] E. F. van Dishoeck[2,3] and H. Linnartz[1]

[1]*Raymond & Beverly Sackler Laboratory for Astrophysics, Leiden Observatory, Leiden University, PO Box 9513, 2300 RA Leiden, the Netherlands*
[2]*Leiden Observatory, Leiden University, PO Box 9513, 2300 RA Leiden, the Netherlands*
[3]*Max-Planck-Institut für Extraterrestriche Physik, Giessenbachstrasse 1, D-85741 Garching, Germany*

Accepted 2011 January 5. Received 2010 November 18; in original form 2010 August 19

ABSTRACT

The surface formation of CO_2 at low temperatures through the reaction CO + OH and direct dissociation of the resulting HO–CO complex is shown by hydrogenation of a CO:O_2 ice mixture. Such a binary ice is not fully representative for an interstellar ice, but the hydrogenation of O_2 ice produces OH radicals, which allows the investigation of the interstellar relevant CO + OH solid state reaction under fully controlled laboratory conditions. Similar recent astrophysical ice studies have focused on the investigation of isolated surface reaction schemes, starting from the hydrogenation of pure ices, like solid CO or O_2. For such ices, no CO_2 formation is observed upon H-atom exposure. The hydrogenation of binary ice mixtures presented here allows to investigate for the first time the influence of the presence of other species in the ice on the pure ice reaction shemes. Mixtures of CO:O_2 are deposited on a substrate in an ultra high vacuum setup at low temperatures (15 and 20 K) and subsequently hydrogenated. The ice is monitored by means of Reflection Absorption InfraRed Spectroscopy (RAIRS). Results show that solid CO_2 is formed in all studied CO:O_2 mixtures under our laboratory conditions. Within the experimental uncertainties no dependency on ice temperature or composition is observed. The laboratory results show a correlation between the formation of CO_2 and H_2O, which is consistent with the astronomical observation of solid CO_2 in water-rich environments. The results also show that the contemporary presence of CO and O_2 molecules in the ice influences the final product yields of the separate CO + H (H_2CO, CH_3OH) and O_2 + H (H_2O_2 and H_2O) channels, even though the formation rates are not significantly affected.

Key words: astrochemistry – methods: laboratory – ISM: atoms – ISM: molecules – infrared: ISM.

1 INTRODUCTION

Infrared Space Observatory and *Spitzer Space Telescope* observations have shown that H_2O, CO, CO_2 and, in some cases, CH_3OH represent the bulk of solid-state species in dense molecular clouds and star-forming regions. Other ice components, such as CH_4, NH_3, OCN^-, H_2CO, HCOOH, SO_2 and OCS have abundances <5 per cent relative to H_2O (e.g. Gibb et al. 2004; Boogert et al. 2008; Pontoppidan et al. 2008; Öberg et al. 2008; Zasowski et al. 2009; Bottinelli et al. 2010). Several of these species are assumed to be formed in solid state reactions on the surfaces of icy dust grains, as outlined by Tielens & Hagen (1982). Although these reactions have been postulated nearly 30 yr ago, few have been measured in the laboratory at low temperatures and under ultra high vacuum (UHV) conditions until recently. Over the past decade, detailed laboratory experiments have started to investigate isolated surface reaction schemes, starting from the hydrogenation of simple and pure ices, like solid CO or O_2.

Several groups proved that the hydrogenation of CO ice at low temperatures (12–20 K) leads to the subsequent formation of H_2CO and CH_3OH (e.g. Watanabe et al. 2004, 2006; Fuchs et al. 2009). The experiments showed that this hydrogenation process involves only the upper monolayers (∼4 ML, where 1 ML corresponds to 10^{15} molecules cm^{-2}) of the CO ice and formation rates drop at temperatures higher than 15 K, since the desorption of H atoms becomes important at these temperatures. The hydrogenation of CO to CH_3OH proceeds in four steps,

$$\mathrm{CO} \xrightarrow{\mathrm{H}} \mathrm{HCO} \xrightarrow{\mathrm{H}} \mathrm{H_2CO} \xrightarrow{\mathrm{H}} \mathrm{H_3CO} \xrightarrow{\mathrm{H}} \mathrm{CH_3OH}, \quad (1)$$

where the first step from CO to HCO and the third step from H_2CO to H_3CO have a barrier.

⋆E-mail: ioppolo@strw.leidenuniv.nl

The other surface reaction channel that has been well investigated is the hydrogenation of O_2 ice, which leads to the formation of H_2O_2 and H_2O (e.g. Ioppolo et al. 2008, 2010; Miyauchi et al. 2008; Cuppen et al. 2010). This hydrogenation process

$$O_2 \xrightarrow{2H} H_2O_2 \xrightarrow{2H} 2H_2O \quad (2)$$

behaves differently compared to the hydrogenation of CO ice (reaction scheme 2 shows the simplified version of this route, as discussed by Tielens & Hagen 1982). In this case, the penetration depth of H atoms in the O_2 ice increases with temperature, even at values close to the desorption temperature of the O_2 layer, involving the bulk of the ice (tens of monolayers). Thus, H atoms trapped in the ice can diffuse and eventually react up to much higher temperatures. Moreover, at least the formation of H_2O_2 does not exhibit any noticeable barrier.

The present work is a further step towards a laboratory investigation of interstellar relevant surface reactions in more complex ices by studying for the first time the formation of solid CO_2 through hydrogenation of a binary CO:O_2 ice mixture as well as investigating the competition between the two separate hydrogenation channels (CO + H and O_2 + H).

CO_2 is one of the most common and abundant ices (d'Hendecourt & Jourdain de Muizon 1989), yet its formation routes are still uncertain. It is widely accepted that CO_2 is not formed efficiently in the gas phase, with subsequent accretion on to the grains ($CO_2^{gas}/CO_2^{ice} \ll 1$; van et al. 1996; Boonman et al. 2003). Therefore, the observed CO_2 most likely has to be formed in the solid phase. Several reaction mechanisms have been proposed with an efficiency depending on astronomical environment. Energetic processing, such as UV and ion irradiation of interstellar ice analogues, has been investigated in various laboratories and proposed as an efficient CO_2 formation mechanism (e.g. Hagen, Allamandola & Greenberg 1979; Mennella, Palumbo & Baratta 2004; Loeffler et al. 2005; Mennella et al. 2006; Ioppolo et al. 2009). Furthermore, in the absence of UV irradiation, several cold solid-phase reaction channels have been reported in the past decades as an alternative formation mechanism to explain the CO_2 abundance observed in cold clouds (e.g. Tielens & Hagen 1982; d'Hendecourt et al. 1985; Grim & d'Hendecourt 1986; Ruffle & Herbst 2001; Fraser & van Dishoeck 2004; Stantcheva & Herbst 2004; Goumans, Uppal & Brown 2008; Goumans & Andersson 2010). The most straightforward surface reaction channel is the addition of an O atom to solid CO ice. The reaction CO + O → CO_2 has been experimentally investigated only by temperature programmed desorption experiments using thermal O atoms below 160 K (Roser et al. 2001) and by energetic O atoms (Madzunkov et al. 2006). This surface reaction channel has a high reaction barrier (Grim & d'Hendecourt 1986), because the CO($^1\Sigma$) + O(^{3}P) reactants do not correlate directly with the singlet ground state $CO_2(^1\Sigma)$ (2970 K in the gas phase; Talbi, Chandler & Rohl 2006). Ruffle & Herbst (2001) found in their astrochemical model that they were only able to reproduce the CO_2 abundances observed towards the cold (10 K) cloud Elias 16, if they artificially lowered the barrier to 130 K. Recently, Goumans & Andersson (2010) used harmonic quantum transition state theory to conclude that whilst quantum mechanical tunnelling through the activation barrier increases the classical reaction rate for reaction CO + O at low temperatures (10–20 K), the onset of tunnelling is at too low temperatures for the reaction to efficiently contribute to CO_2 formation in quiescent clouds.

Solid CO_2 is further suggested to be formed through the surface reaction HCO + O, which presents two exit channels (CO_2 + H and CO + OH; Ruffle & Herbst 2001). Alternatively, solid CO_2 can be formed through the surface reaction CO + OH, which yields a HO–CO intermediate. This complex can directly dissociate, forming solid CO_2 and leaving a H atom, or can be stabilized by intramolecular energy transfer to the ice surface and eventually react with an incoming H atom in a barrierless manner to form CO_2 and H_2 (Goumans et al. 2008).

Fig. 1 shows a schematic representation of all the reaction networks investigated in this work (solid arrows) and links the previously studied CO + H and O_2 + H channels through the observed CO_2 formation. The dashed and dotted arrows represent suggested CO_2 formation routes in the networks of Tielens & Hagen (1982) and Ruffle & Herbst (2001), that are not experimentally confirmed at low temperature in our studies.

In Section 4.1 we discuss that CO_2 is formed under our experimental conditions through the reaction CO + OH. Here OH radicals are formed through the hydrogenation of O_2 ice, while in space they can also result from the O + H reaction or from the photodissociation of H_2O ice. Recently, Oba et al. (2010) also investigated the reaction CO + OH depositing CO molecules on a cold substrate (10 and 20 K) together with H_2O fragments (OH, H, O and H_2) produced by dissociating H_2O molecules in a microwave source. They observed the formation of solid CO_2 at low temperature by using CO and OH beams to initiate surface reactions on a cold substrate. Their experiments differ from ours. In the present work, we hydrogenate CO:O_2 ices and OH radicals are produced in the ice through the O_2 + H channel, providing additional information on the interaction between different surface reaction schemes. In a previous paper (Ioppolo et al. 2011), we investigated experimentally the hydrogenation of the HO–CO complex, which has three exit channels (CO_2 + H_2, HCOOH, H_2O + CO) with a purely statistical branching ratio as suggested by density functional theory models and in agreement with our experimental results (Goumans et al. 2008; Ioppolo et al. 2011). In the present study, the HO–CO complex itself is not observed since it is efficiently dissociated under our experimental conditions to form CO_2. More details are reported in Section 4. In Sections 2 and 3, the experimental method and data analysis are discussed .

2 EXPERIMENTAL DETAILS

The experiments are performed using an UHV setup, which consists of a main chamber (10^{-10} mbar) and an atomic beam line. Details are available from Fuchs et al. (2009) and Ioppolo et al. (2010). The ice is grown on a gold coated copper substrate (12–300 K) that is mounted on the cold head of a close-cycle He cryostat. Deposition of selected $^{12}C^{16}O$:$^{16}O_2$ mixtures (4:1, 1:1 and 1:4) proceeds under an angle of 45° and with a rate of 0.7 ML min^{-1}. After deposition the ice mixture is exposed to a cold H-atom beam. H_2 molecules are dissociated into the capillary of a well-characterized thermal cracking source (Tschersich & von Bonin 1998; Tschersich 2000; Tschersich, Fleischhauer & Schuler 2008), which is used to hydrogenate the sample. A quartz pipe with a nose-shaped form is placed along the path of the dissociated beam to efficiently thermalize all H atoms to room temperature through surface collisions before they reach the ice sample. In this way, hot species (H; H_2) cannot reach the ice directly. Furthermore, the relatively high temperature of 300 K of the incident H atoms in our experiments does not affect the experimental results, since H atoms are thermally adjusted to the surface temperature as has been shown in Fuchs et al. (2009). The final H-atom flux

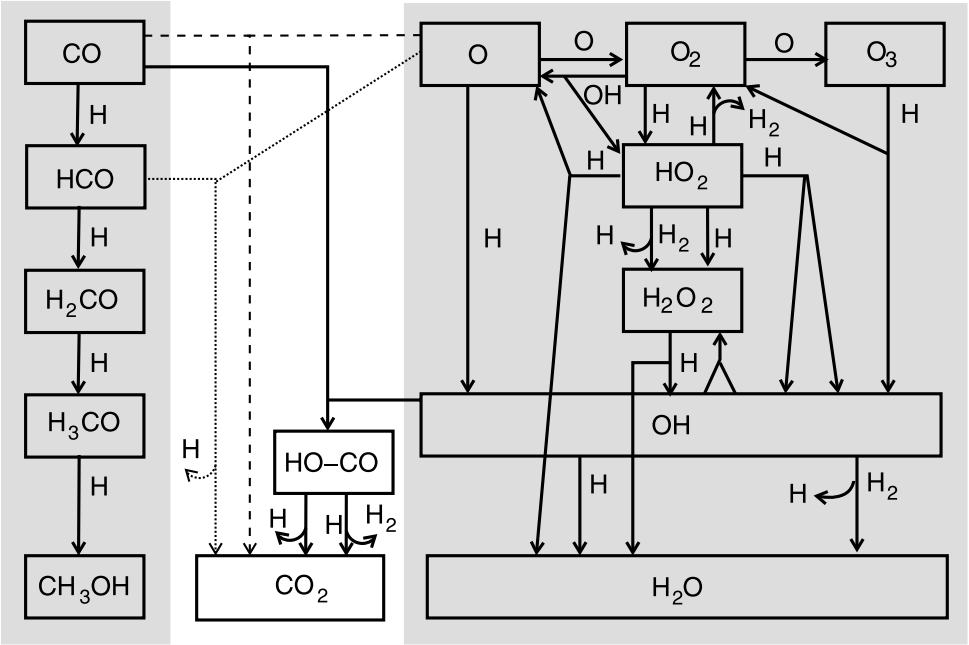

Figure 1. A schematic representation of the reaction network as discussed in the present study. The CO + H channel is shown on the left-hand side of the figure, while the $O/O_2/O_3$ + H channels are plotted as presented in Cuppen et al. (2010) on the right-hand side. The possible CO_2 formation routes are shown in between the CO + H and $O/O_2/O_3$ + H channels: the dissociation of the HO–CO intermediate (solid arrow) is one of the topics of this work; the hydrogenation of the HO–CO complex (solid arrow) is presented in Ioppolo et al. (2011); the suggested CO + O (dashed arrow) and HCO + O (dotted arrow) routes are not experimentally confirmed at low temperature (Tielens & Hagen 1982; Ruffle & Herbst 2001).

(2.5×10^{13} atoms $cm^{-2}\,s^{-1}$) is measured at the substrate position in the main chamber using a quadrupole mass spectrometer, following the procedure as described in the appendix of Ioppolo et al. (2011). The error in the absolute H-atom flux determination is within 50 per cent. Ices are monitored by means of Reflection Absorption InfraRed Spectroscopy (RAIRS) using a Fourier Transform InfraRed spectrometer (FTIR), which covers the range between 4000 and 700 cm^{-1} (2.5–14 μm). A spectral resolution of 1 cm^{-1} is used and 128 scans are co-added for one spectrum. RAIR difference spectra (ΔA) relative to the initial unprocessed $CO:O_2$ ice are acquired every few minutes during H-atom exposure.

We performed a control experiment at 15 K in which a $CO:O_2$ ice is exposed to an H_2 molecular beam (i.e. without H atoms) to show that the products detected in the hydrogenation experiments are formed on the surface and do not originate from background deposition. Only small amounts of H_2O are detected in this experiment, which gives us an estimate for the background contamination, which is negligible. None of the other products is detected in this way. The present experiments use the same H-atom flux as adopted in Fuchs et al. (2009) and Ioppolo et al. (2011). Therefore, the hydrogenation of our mixtures involves effectively a lower H-atom flux per (CO + H and O_2 + H) reaction channel.

The interstellar solid $CO:O_2$ mixing ratio is observationally constrained to >1:1 (e.g. Vandenbussche et al. 1999; Pontoppidan et al. 2003). This conclusion was deduced earlier by d'Hendecourt et al. (1985) on the basis of a simple interacting gas-phase/solid-phase time-dependent model. In our experiments, the binary mixture ratios ($CO:O_2$ = 4:1, 1:1 and 1:4) are selected to efficiently produce thermal OH radicals in the ice in order to investigate the formation of CO_2. These experiments are also meant to test the interaction of the aforementioned individual surface reaction channels, rather than simulating a complete realistic interstellar ice evolution.

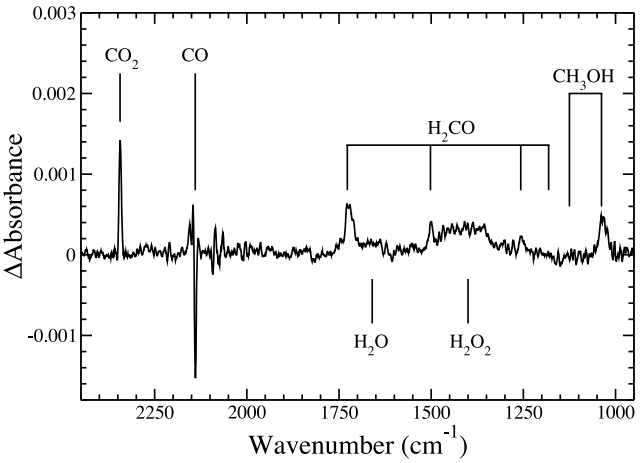

Figure 2. RAIR difference spectrum of the $CO:O_2$ = 1:4 ice, with respect to the spectrum before H-atom addition, at 15 K after a H-atom fluence of 1.3×10^{17} atoms cm^{-2}.

3 DATA ANALYSIS

Fig. 2 shows a RAIR difference spectrum of a $CO:O_2$ = 1:4 mixture acquired after a H-atom fluence (flux × time) of 1.3×10^{17} atoms cm^{-2}. The negative peak shown in Fig. 2 is caused by the CO use-up in surface reaction processes. O_2 is infrared inactive and therefore cannot be observed in this spectrum. All the final reaction products obtained from the hydrogenation of a pure CO ice (H_2CO and CH_3OH; e.g. Watanabe et al. 2004, 2006; Fuchs et al. 2009) and a pure O_2 ice (H_2O and H_2O_2; e.g. Ioppolo et al. 2008; Miyauchi et al. 2008) are present. Neither the intermediate species from the separate CO and O_2 channels, like HCO, H_3CO, HO_2, OH and O_3,

nor more complex species, like the stabilized HO–CO intermediate, HCOOH and H_2CO_3,[1] are observed as was the case in experiments by Ioppolo et al. (2011) in which the CO:O_2 mixtures and H atoms were deposited simultaneously. However, a new feature appears at $\sim$2344 cm^{-1}, which belongs to the asymmetrical stretching mode of CO_2 ice. This molecule is formed in all our performed experiments at 15 and 20 K, with different CO:O_2 mixing ratios, but was not found in the previous CO + H or O_2 + H experiments.

The infrared spectra are reduced to obtain the column densities of the newly formed species. As a first step in the infrared data analysis, a straight baseline is subtracted from all spectra. Some absorption features, like the H_2O bending mode ($\sim$1650 cm^{-1}) and the H_2CO ν(CO) stretching mode ($\sim$1720 cm^{-1}) suffer from spectral overlap. Here a multi-Gaussian fit is used to determine the area of the selected bands. Since the asymmetric 1440 cm^{-1} H_2O_2 band overlaps with the 1500 cm^{-1} H_2CO band, a spectrum of pure H_2O_2 ice is fitted in addition to a Gaussian. The spectrum of solid H_2O_2 is obtained as discussed by Cuppen et al. (2010), by co-depositing H atoms and O_2 molecules with a ratio of H/O_2 = 20 and subsequently heating the ice to a temperature higher than 30 K, which is just above the O_2 desorption temperature (Acharyya et al. 2007).

The column density N_X (molecules cm^{-2}) of species X in the ice is calculated using: $N_X = \int A(\nu)\,\mathrm{d}\nu / S_X$, where $A(\nu)$ is the wavelength-dependent absorbance. Since literature values of transmission band strengths cannot be used in reflection measurements, an apparent absorption band strength, S_X of species X, is determined by individual calibration experiments. These have been described in detail in Fuchs et al. (2009), Ioppolo et al. (2010) and Cuppen et al. (2010). Like for CO, CH_3OH and H_2O, an isothermal desorption experiment has been performed to determine the apparent absorption band strength of CO_2 by determining the transition from zeroth-order to first-order desorption. This is assumed to occur at the onset to the submonolayer regime and appears in the desorption curve as a sudden change in slope. Since pure H_2CO and H_2O_2 are experimentally difficult to deposit, because of their chemical instability, the values for S_{H_2CO} and $S_{H_2O_2}$ are obtained by assuming mass balance as reported in Fuchs et al. (2009) and Cuppen et al. (2010), respectively.

4 RESULTS AND DISCUSSION

4.1 Formation of solid CO_2

Fig. 3 shows the CO_2 column density as a function of the H-atom fluence, confirming the CO_2 formation for the three different mixing ratios and two temperatures investigated. Here neither the CO_2 formation rate nor its final yield depends significantly on either temperature or mixing ratio for the studied values. Such a behaviour is unexpected, since the separate reaction routes CO + H and O_2 + H clearly depend on temperature, as shown by Fuchs et al. (2009) and Ioppolo et al. (2010). The limiting factor for the CO_2 synthesis in our experiments is, therefore likely, the amount of ice that can be penetrated by H atoms, which is only a few monolayers. This is caused by the presence of CO molecules affecting the penetration depth of the H atoms in the ice (Fuchs et al. 2009). Thus, the amount of CO_2 formed in all our experiments is always less than a monolayer. CO_2 subsequently does not contribute to further molecular synthesis in the ice upon ongoing hydrogenation. Bisschop et al. (2007) showed

[1] Solid H_2CO_3 was observed only in control experiments by Ioppolo et al. (2011).

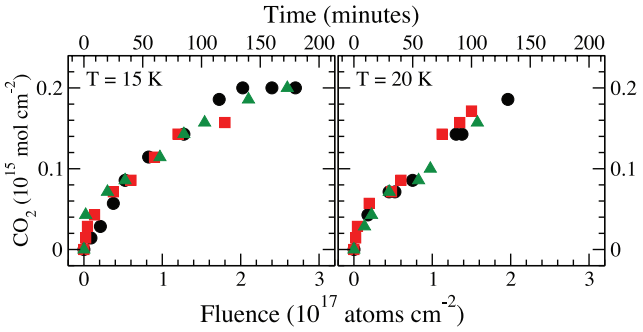

Figure 3. CO_2 column density as a function of the H-atom fluence and time of H-atom exposure at 15 K (left) and 20 K (right) for the three mixtures studied: CO:O_2 = 4:1 (circle), 1:1 (square), and 1:4 (triangle).

experimentally that CO_2 does not react with H atoms and is a stable molecule under interstellar ice analogue conditions.

Fig. 1 summarizes schematically the reaction network which leads to the formation of solid CO_2 starting from the combination of the CO + H and O_2 + H channels. Analysing the species present in our ice after H-atom addition, we can identify which reaction channel is most likely responsible for the formation of solid CO_2 ice. The hydrogenation of the HO–CO intermediate (black arrow in the centre of Fig. 1) should not occur in our experiments, since HCOOH is not detected in the infrared spectra. Density functional calculations (Goumans et al. 2008), confirmed by our previous experimental results (Ioppolo et al. 2011), suggest that the final products from the hydrogenation of the HO–CO complex have a purely statistical branching ratio. Therefore, HCOOH should be detected in the ice if CO_2 would be produced through this route, and this is not the case.

The oxidation of solid CO (dashed arrow) is also not likely to be the main formation reaction channel, since O_3, which would indirectly prove the presence of abundant O atoms in the ice, is not observed. O_3 ice has been detected in pure O_2 hydrogenation experiments only for temperatures higher than 25 K, when the penetration depth of the H atoms is higher than a few monolayers and the O_2 molecules are most likely more mobile (Ioppolo et al. 2010). The hydrogenation of O_3 ice (studied in Romanzin et al. 2011) is therefore not considered here. Furthermore, Roser et al. (2001) tentatively observed CO_2 formation through this channel only during the warm up of the ice and when CO molecules and O atoms were covered by a thick layer of H_2O ice, which allows the reactants to remain trapped in the ice for $T > 100$ K. The CO + O reaction contributes at best at high temperatures. The reaction HCO + O (dotted arrow) should also be ruled out, since HCO radicals prefer to react in a barrierless manner with H atoms forming H_2CO rather than with O atoms, as shown by Fuchs et al. (2009) and Ioppolo et al. (2011). Furthermore, as stated before, O atoms are not abundant in our ices.

At low temperatures, CO_2 is likely formed through the direct dissociation of the HO–CO complex in the ice (black arrow). The HO–CO complex is efficiently dissociated and, therefore, is not detected in our infrared spectra as a stable species. In a previous paper (Ioppolo et al. 2011), we observed this complex only in a water-rich environment. H-bonding should, indeed, improve coupling and heat dissipation through the ice, which stabilizes the HO–CO complex more easily in a polar than in an apolar environment. Our ice is mainly composed of CO and O_2, with a polar component on the surface of the ice. The amount of the HO–CO intermediate stabilized in the polar ice is also under the detection limit. Therefore, in a water-poor ice, the competition between dissociation and further

hydrogenation of the HO–CO complex is in favour of the dissociation.

H_2O is also formed through hydrogenation of the OH radicals (Fig. 2). Hence, the formation of CO_2 is linked to the formation of H_2O in the ice. This is consistent with the presence of CO_2 in polar (water-rich) interstellar ice mantles (see discussion in Section 5).

4.2 Hydrogenation of O_2 molecules

In this section, we investigate to what extent the hydrogenation of O_2, previously studied also for a pure ice, is affected by the presence of other molecules. Fig. 4 shows the H_2O_2 (top panels) and H_2O (bottom panels) column densities as a function of the H-atom fluence for the three different mixing ratios [CO:O_2 = 4:1 (circles), 1:1 (squares) and 1:4 (triangles)] and two temperatures investigated [15 K (left-hand panels) and 20 K (right-hand panels)]. For comparison, results from the hydrogenation of pure O_2 ice (Ioppolo et al. 2010) are also plotted (diamonds). Note that the top-right panel has a different scale for the column density axis than the other three diagrams. Formation rate and final yield of H_2O_2 and H_2O for all the investigated mixtures are lower than those from the pure O_2 ice hydrogenation. The differences in the final yield are more evident at higher temperature, where the yield for the mixed ices only moderately increases, whereas it increases with several monolayers for the pure O_2 experiments. This cannot be explained only by a low effective H-atom flux for the O_2 channel. Hence, the presence of CO in the mixture influences the final results. In a previous paper on CO + H we showed that H atoms can penetrate only a few layers of CO ice (Fuchs et al. 2009). Therefore, the presence of CO in the mixture most likely diminishes the penetration depth of H atoms into the ice compared to O_2 + H, and, therefore, desorption of H atoms from the ice can become important at higher temperatures. This explains the difference in the H_2O_2 and H_2O final yields compared to those from the pure O_2 ice, which increases with temperature.

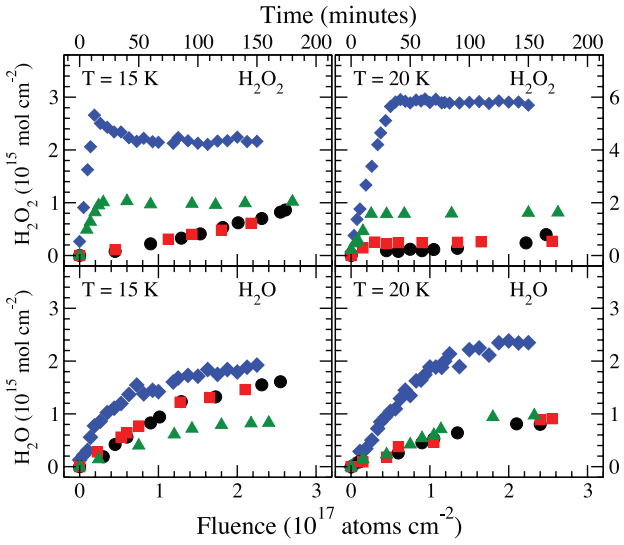

Figure 4. H_2O_2 (top panels) and H_2O (bottom panels) column densities as a function of the H-atom fluence and time of H-atom exposure at 15 K (left-hand panels) and 20 K (right-hand panels) for the three mixtures studied: CO:O_2 = 4:1 (circle), 1:1 (square) and 1:4 (triangle). For comparison, results from the hydrogenation of pure O_2 ice are plotted (diamond). Note the different vertical scale for upper right-hand panel.

The formation rates of H_2O and H_2O_2, which are reflected by the initial slopes of the curves, are also altered by the presence of CO in the ice. In the O_2-rich ice (1:4), the H_2O_2 column density shows the same behaviour as seen in pure O_2 ices: a constant formation rate is followed by a sharp transition towards saturation (Ioppolo et al. 2010). For high concentration of CO in the ice, the H_2O_2 column density increases with a much lower rate and does not appear to reach a steady state, even at the highest fluence. The H_2O_2 final yield increases with temperature, like for hydrogenation experiments of pure O_2 ice.

In the case of CO-rich ice (4:1), a more efficient conversion of H_2O_2 ice into H_2O ice can explain the high H_2O final yield with respect to the O_2-rich ice experiment. In a previous paper, we showed that H_2O_2 is more effectively formed in the bulk of the ice (Ioppolo et al. 2010). However, the presence of CO in the ice restricts the hydrogenation reactions to the surface of the ice. This means that a larger percentage of H_2O_2 formed at the surface of the ice is easily converted into H_2O. This may also explain the lower effective synthesis of H_2O_2 with the increase of the number of CO molecules in the ice. In addition, H_2O can be formed from OH radicals (see Fig. 1 and Cuppen et al. 2010), which can also react to form CO_2 in our ices. The H_2O column density is constant through almost all our experiments. This is also the case for CO_2 as shown in Section 4.1 and indicative for a correlation between the formation channels of these two species.

4.3 Hydrogenation of CO molecules

Fig. 5 shows the H_2CO (top panels) and CH_3OH (bottom panels) column densities as a function of the H-atom fluence for the three different mixing ratios [CO:O_2 = 4:1 (circles), 1:1 (squares) and 1:4 (triangles)] and two temperatures investigated [15 K (left-hand panels) and 20 K (right-hand panels)]. For comparison, results from the hydrogenation of pure CO ice (Fuchs et al. 2009) are also plotted (diamonds). For the hydrogenation of pure CO ice, the H-atom fluence is corrected according to recent H-atom flux measurements (Ioppolo et al. 2010), which improve the original H-atom flux

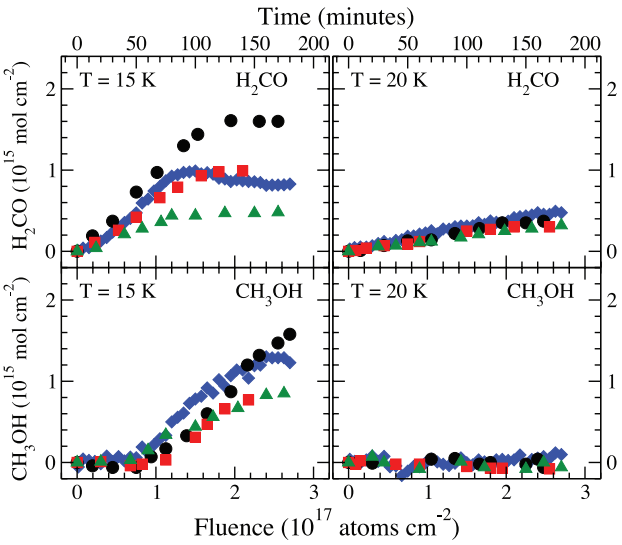

Figure 5. H_2CO (top panels) and CH_3OH (bottom panels) column densities as a function of the H-atom fluence and time of H-atom exposure at 15 K (left-hand panels) and 20 K (right-hand panels) for the three mixtures studied: CO:O_2 = 4:1 (circle), 1:1 (square) and 1:4 (triangle). For comparison, results from the hydrogenation of pure CO ice are plotted (diamond).

estimation derived in Fuchs et al. (2009). The hydrogenation of CO molecules in our mixtures shows the same behaviour seen for pure CO ice in terms of temperature dependence (Fuchs et al. 2009). An optimum in the final yield for H_2CO and CH_3OH is found at 15 K, while at 20 K no CH_3OH is formed and H_2CO has a low formation rate. The H_2CO and CH_3OH formation rates are hardly affected by the presence of O_2 in the ice (within the experimental uncertainties). The higher final yield for H_2CO and CH_3OH in the CO:O_2 = 4:1 experiment at 15 K compared to the pure CO ice cannot be explained by only a difference in the effective H-atom flux. In this case, the presence of O_2 in the ice, as a minor component, increases the penetration depth of H atoms in the ice compared to pure CO and, therefore, the probability that the H atoms get trapped and react in the ice. However, if the O_2 concentration is increased in the 15 K ice, the final yield decreases for both H_2CO and CH_3OH molecules. Clearly, the formation of H_2CO is more sensitive to the O_2 concentration in the ice than the formation of CH_3OH. As we saw for the hydrogenation of O_2 ice, the intermediate products (H_2O_2 and H_2CO, respectively) are more efficiently converted in the final products (H_2O and CH_3OH, respectively), when the ices are mixed.

4.4 Competition between the CO and O_2 channel

The results presented in the former sections reflect the competition between the two channels CO versus O_2, as shown in the left and right part of Fig. 1. It is clear from the experimental results that the presence of one component in the ice influences the reactivity of the other component. The formation rate of the CO hydrogenation reaction products is less affected by the presence of O_2 than the O_2 hydrogenation reaction products are affected by the presence of CO. This can be explained by the lower penetration depth of H atoms in CO ice and by the formation of CO_2 as an additional product, since OH radicals, formed through the O_2 channel, are used to form CO_2 instead of H_2O and H_2O_2.

In a CO-rich environment at 15 K, the presence of O_2 molecules enhances the production of H_2CO and CH_3OH, since H atoms can penetrate deeper in the ice than in the pure CO ice experiment. However, the formation rate of the final products seems not to be affected by the presence of the O_2 molecules in the ice. Moreover in a CO-rich ice, the formation of H_2O_2 is limited by the small amount of O_2 molecules in the ice, by the amount of OH radicals used to form CO_2 and by the lower penetration depth of H atoms in the ice, caused by the presence of CO molecules. H_2O_2 ice is also more efficiently converted to H_2O on the surface of the ice. This explains the high final yield for H_2O in a CO-rich environment at 15 K.

In a O_2-rich environment at 15 K, the formation of H_2CO and CH_3OH is limited by the small amount of CO molecules, which limits the formation of H_2O_2 and H_2O, since the penetration depth of H-atoms is lower than in the pure O_2 ice experiment.

At 20 K, the CO channel is not efficient, although the H atoms penetrate deep in the ice; at this temperature H atoms prefer to react with O_2 molecules. Also in this case, the final yields for H_2O_2 and H_2O are lower than those in the pure O_2 ice experiment.

5 ASTROPHYSICAL IMPLICATIONS

Observations by the *Infrared Space Observatory* (e.g. Gerakines et al. 1999; Nummelin et al. 2001; Gibb et al. 2004) and the *Spitzer Space Telescope* (e.g. Boogert et al. 2004; Bergin et al. 2005; Pontoppidan et al. 2005; Pontoppidan 2006; Whittet et al. 2007; Pontoppidan et al. 2008) have shown that roughly two-third of the solid CO_2 observed in quiescent molecular clouds and star-forming regions is found in water-rich environments, suggesting that the formation routes of these two molecules are linked. The remaining CO_2 ice is predominantly found in a H_2O-poor, CO-rich environment (Pontoppidan et al. 2008). These observations suggest that the formation of CO_2 in dark quiescent clouds occurs in two distinct phases. In the early stages, CO_2 forms together with H_2O on the surface of the interstellar dust grains, creating a polar ice mantle. A second phase in the CO_2 formation occurs during the heavy freeze-out of CO. During this second phase, a H_2O-poor ice is formed.

Our experimental results indeed make it likely that CO_2 and H_2O are formed together in the early stages of the clouds through surface reactions assuming that both CO and OH are present in sufficiently high abundances. H_2O ice forms from continued hydrogenation of OH radicals formed on the surface of the dust grains. Alternatively, OH radicals can react with nearby CO molecules, which are present in small amounts in the ice before the strong CO freeze-out phase, forming CO_2 ice through the direct dissociation of the HO–CO intermediate. CO_2 can be also formed at low temperatures through the hydrogenation of the HO–CO complex, which can lead to the formation of HCOOH and H_2O + CO as well as CO_2 + H_2. The concentration of CO in the ice with respect to H atoms determines the probability of OH to react with a CO molecule or with another H atom.

In the second stage, during the heavy CO freeze-out, the gas density is $>10^5$ cm^{-3} and the CO accretion rate could be as high as, or even higher than, the H-atom accretion rate, which makes CO more abundant on the surface than H atoms. Any OH radicals will therefore more likely react with a nearby CO molecule than with H atoms. As long as some OH is present, CO_2 can thus be efficiently formed through the dissociation or further hydrogenation of the HO–CO complex, while just little H_2O ice is formed.

Energetic processing (UV irradiation and cosmic ray-induced photons) of polar and apolar ices is another efficient mechanism for CO_2 formation for specific (water-rich) environments (e.g. Hagen et al. 1979; Mennella et al. 2004, 2006; Loeffler et al. 2005; Ioppolo et al. 2009). All these channels, including the scheme discussed here, can contribute to the total CO_2 column density component observed in quiescent clouds.

In addition, in our experiments only a small amount of H_2O_2 ice is formed. This work shows that the competition between different channels (CO + H and O_2 + H), together with the penetration depth of the incoming H atoms into the ice, which decreases when the amount of CO in the ice increases, explains the differences in the H_2O_2 and H_2O final yield between a mixed and pure O_2 ice. Our results are consistent with the observed lack of H_2O_2 in the interstellar ices.

6 CONCLUSIONS

The experiments presented here show that CO_2 can be formed in the solid state for astronomically relevant temperatures via a thermal CO + OH reaction path. An efficient dissociation of the HO–CO complex is observed and this may explain the presence of CO_2 in polar and apolar interstellar ices in absence of UV irradiation. For the investigated laboratory conditions, CO_2 is formed efficiently and no strong dependency on temperature or ice composition is found. It is explicitly stated here that this conclusion does not rule out other CO_2 formation routes in space. Fig. 1, for example, shows how the H_2O formation through the $O/O_2/O_3$ + H channels is linked to the CO_2 formation. Here we investigated only the O_2 + H channel, and it should be noted that OH radicals can be also efficiently formed

on dust grains through the other H_2O formation channels as well as through the photodissociation of H_2O and CH_3OH ice.

The formation of CO_2 is linked to the formation of H_2O and, therefore, competes with the O_2 hydrogenation channel in our experiments. The competition of the two channels, together with the composition of the ice and the penetration depth of H atoms into the ice, explains the differences in the H_2O_2 and H_2O formation rate between a mixed and pure O_2 ice. Also the CO + H and O_2 + H channels are in competition and clearly affect each others final product yields. This is consistent with the lack of observed H_2O_2 in the interstellar ices. The formation rate for all the final products is found to be less sensitive on the mixture composition than the final yield. The penetration depth of the incoming H atoms is the main limiting factor. It depends on the composition of the ice and decreases when the amount of CO in the ice increases. Our results show that the formation rates found for H_2CO, CH_3OH, H_2O_2 and H_2O are similar within their experimental uncertainties to those found for the isolated CO and O_2 hydrogenation channels (corrected for the reduced effective H-atom fluxes). Those values, therefore, are still valid for use in astrochemical models. Finally, the experiments presented here chemically link CO_2 and H_2O, consistent with the observation of CO_2 in H_2O-rich environments in space.

ACKNOWLEDGMENTS

The research leading to these results has received funding from NOVA, the Netherlands Research School for Astronomy, a Spinoza grant from the Netherlands Organisation for Scientific Research, NWO, and the European Community's Seventh Framework Programme (FP7/2007-2013) under grant agreement n°238258.

REFERENCES

Acharyya K., Fuchs G. W., Fraser H. J., van Dishoeck E. F., Linnartz H., 2007, A&A, 466, 1005
Bergin E. A., Melnick G. J., Gerakines P. A., Neufeld D. A., Whittet D. C. B., 2005, ApJ, 627, L33
Bisschop S. E., Fuchs G. W., van Dishoeck E. F., Linnartz H., 2007, A&A, 474, 1061
Boogert A. C. A. et al., 2004, ApJS, 154, 359
Boogert A. C. A. et al., 2008, ApJ, 678, 985
Boonman A. M. S., van Dishoeck E. F., Lahuis F., Doty S. D., 2003, A&A, 399, 1063
Bottinelli S. et al., 2010, ApJ, 718, 1100
Cuppen H. M., Ioppolo S., Romanzin C., Linnartz H., 2010, Phys. Chem. Chem. Phys., 12, 12077
d'Hendecourt L. B., Jourdain de Muizon M., 1989, A&A, 223, L5
d'Hendecourt L. B., Allamandola L. J., Greenberg J. M., 1985, A&A, 152, 130
Fraser H. J., van Dishoeck E. F., 2004, Advances Space Res., 33, 14
Fuchs G. W., Cuppen H. M., Ioppolo S., Bisschop S. E., Andersson S., van Dishoeck E. F., Linnartz H., 2009, A&A, 505, 629
Gerakines P. A. et al., 1999, ApJ, 522, 357
Gibb E. L., Whittet D. C. B., Boogert A. C. A., Tielens A. G. G. M., 2004, ApJS, 151, 35
Goumans T. P. M., Andersson S., 2010, MNRAS, 406, 2213
Goumans T. P. M., Uppal M. A., Brown W. A., 2008, MNRAS, 384, 1158
Grim R. J. A., d'Hendecourt L. B., 1986, A&A, 167, 161
Hagen W., Allamandola L. J., Greenberg J. M., 1979, Ap&SS, 65, 215
Ioppolo S., Cuppen H. M., Romanzin C., van Dishoeck E. F., Linnartz H., 2008, ApJ, 686, 1474
Ioppolo S., Palumbo M. E., Baratta G. A., Mennella V., 2009, A&A, 493, 1017
Ioppolo S., Cuppen H. M., Romanzin C., van Dishoeck E. F., Linnartz H., 2010, Phys. Chem. Chem. Phys., 12, 12065
Ioppolo S., Cuppen H. M., van Dishoeck E. F., Linnartz H., 2011, MNRAS, 410, 1089
Loeffler M. J., Baratta G. A., Palumbo M. E., Strazzulla G., Baragiola R. A., 2005, A&A, 435, 587
Madzunkov S., Shortt B. J., MacAskill J. A., Darrach M. R., Chutjian A., 2006, Phys. Rev. A, 73, 02091
Mennella V., Palumbo M. E., Baratta G. A., 2004, ApJ, 615, 1073
Mennella V., Baratta G. A., Palumbo M. E., Bergin E. A., 2006, ApJ, 643, 923
Miyauchi N., Hidaka H., Chigai T., Nagaoka A., Watanabe N., Kouchi A., 2008, Chem. Phys. Lett., 456, 27
Nummelin A., Whittet D. C. B., Gibb E. L., Gerakines P. A., Chiar J. E., 2001, ApJ, 558, 185
Oba Y., Watanabe N., Kouchi A., Hama T., Pirronello V., 2010, ApJ, 712, L174
Öberg K. I., Boogert A. C. A., Pontoppidan K. M., Blake G. A., Evans N. J., Lahuis F., van Dishoeck E. F., 2008, ApJ, 678, 1032
Pontoppidan K. M., 2006, A&A, 453, L47
Pontoppidan K. M. et al., 2003, A&A, 408, 981
Pontoppidan K. M., Dullemond C. P., van Dishoeck E. F., Blake G. A., Boogert A. C. A., Evans N. J., II, Kessler-Silacci J. E., Lahuis F., 2005, ApJ, 622, 463
Pontoppidan K. M. et al., 2008, ApJ, 678, 1031
Romanzin C., Ioppolo S., Cuppen H. M., van Dishoeck E. F., Linnartz H., 2011, J. Chem. Phys., in press
Roser J. E., Vidali G., Manicò G., Pirronello V., 2001, ApJ, 555, L61
Ruffle D. P., Herbst E., 2001, MNRAS, 324, 1054
Stantcheva T., Herbst E., 2004, A&A, 423, 241
Talbi D., Chandler G. S., Rohl A. L., 2006, Chem. Phys., 320, 214
Tielens A. G. G. M., Hagen W., 1982, A&A, 114, 245
Tschersich K. G., 2000, J. Appl. Phys., 87, 2565
Tschersich K. G., von Bonin V., 1998, J. Applied Phys., 84, 4065
Tschersich K. G., Fleischhauer J. P., Schuler H., 2008, J. Applied Phys., 104, 034908
van Dishoeck E. F. et al., 1996, A&A, 315, L349
Vandenbussche B. et al., 1999, A&A, 346, L57
Watanabe N., Nagaoka A., Shiraki T., Kouchi A., 2004, ApJ, 616, 638
Watanabe N., Nagaoka A., Hidaka H., Shiraki T., Chigai T., Kouchi A., 2006, Planetary Space Sci., 54, 1107
Whittet D. C. B., Shenoy S. S., Bergin E. A., Chiar J. E., Gerakines P. A., Gibb E. L., Melnick G. J., Neufeld D. A., 2007, ApJ, 655, 332
Zasowski G., Kemper F., Watson D. M., Dan M., Furlan E., Bohac C. J., Hull C., Green J., 2009, ApJ, 694, 459

This paper has been typeset from a TEX/LATEX file prepared by the author.